International Journal of Scientific Research in Engineering and Management (IJSREM)
Volume: 06 Issue: 07 | July - 2022 Impact Factor: 7.185 ISSN: 2582-3930

Design Optimization and Analysis of Steering and Braking Sub-System of a Go-Kart

K.V. Praveen[1], S. Abdul Azeez[2], G. Vamsi[3], K. Durga Prasad[4], K. Vamsi[5]

[1,2,3,4,5] Department of Mechanical Engineering, Raghu Engineering College (A), Visakhapatnam-531162.

---***---

Abstract - The Go-Kart is a four-wheeled racing car without a differential or suspension. There are several different types of go-karts, ranging from non-motorized models to extremely fast racing karts. The two primary control systems of a go-kart are the steering system and the braking system. Our objectives were to locate design defects, notably in these two sub-systems, and to enhance the design of components such as stub axle and brake disc. This paper gives you an idea and approach under theoretical calculations to design the steering geometry which is a flawless Ackermann mechanism, by optimizing the design of the stub axle and to design an effective braking system, by optimizing the design of the brake disc. The Catia v5 software is used to create the design, and the ANSYS 16.0. software is used to analyze the optimized designs. Based on the results from the analysis, the go-kart is modified to incorporate the new design in the relevant sub-systems.

Key Words: Ackermann steering geometry, stub axle, hydraulic braking, brake disc, CATIA, ANSYS, Structural analysis, Thermal analysis

1. INTRODUCTION

Both steering system and braking system are an important part of the dynamic design of any automobile to facilitate control over a vehicle [1-3]. The steering system enables a vehicle for its smooth change of directions and makes use of the tires ability to generate lateral forces to the highest extent. The sensory inputs of a racing driver provide visual, tactile, and inertial information that is utilized to create a "feel" for the handling and performance of the car. It also acts as a feedback device that informs the driver about the vehicle's stability and steering control [4-5].

The primary purpose of the vehicle's braking system is to stop or slow it down. This system combines a few interactive components. It absorbs energy from the moving part and slows down the vehicle with the help of friction [6]. The common misconception is that when the brakes apply pressure to a disc, the vehicle slows down as a result.

2. DESIGN METHODOLOGY

Fig -1: Design methodology

3. PROBLEM IDENTIFICATION

3.1 Problems raised in the Steering subsystem

Since the improper design of stub axle and misalignment of components placement, the following problems are raised.

- Understeer
- Long turning radius.
- Bumping of wheels.
- Increase in effort provided to steer the steering wheel.
- Pulling the vehicle to the side on which more weight is acting, when brake applied.

3.2 Problems raised in the braking subsystem

Since the oversize design of the brake disc following problems are raised.

- Required ground clearance is not achieved (above 1inch).
- Increase in weight.

4. STEERING SUBSYSTEM

4.1 Steering geometry

Steering geometry is the geometric arrangement of the parts of a steering system, and the value of the lengths and angles within. As far as the geometry of steering is concerned, Ackermann geometry is selected. Ackermann steering geometry enables the wheels to turn at different angles, the inside wheel steers to a greater angle than the outside wheel and all the wheels roll about a common turn center. Since the cornering speeds are small, Ackermann geometry is an ideal choice.

4.2 Steering calculations

A. Approach

Considering the turning radius of 1.6 m, using the Ackermann equation for the dimensions of our go-kart, the maximum steering angles were calculated.

Wheel Base (L): 1219.2 mm
Turning Radius (R): 1651 mm
Track Width (T): Front = 863.6 mm | Rear = 990.6 mm
Wheel Diameter: Front = 254 mm | Rear = 279.4 mm
Wheel Thickness: Front = 127 mm | Rear = 203.2 mm

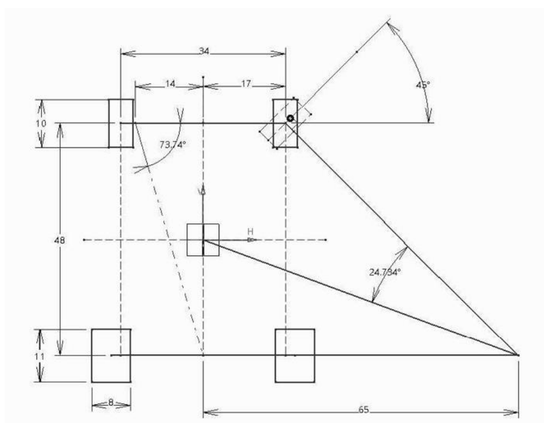

Fig -2: Ackermann steering geometry

1. Ackerman Angle (α):
   α= tan -1 ((0.5*TRACK WIDTH)/WHEELBASE)
   = tan -1 (0.5*863.6/1219.2)
   = tan -1 (431.95/1219.2)
   = tan -1 (0.354)
   = 19.50°
2. Inner Angle:
   Tan B = L/(R+d/2)
   Tan B = 1219/ (1651 + (254/2))
   Tan B = 0.685
   B = Tan -1 (0.685)
   B = 34.43°
3. Outer Angle:
   Tan A = L/(R-d/2)
   Tan A = 1219.2/ (1651 – (254/2))
   Tan A = 0.799
   A = Tan -1 (0.799)
   A = 38.65°
4. Actual Turning Radius:
   = T/2+L Cosec (A/2 + B/2)
   = (863.6/2) + 1219.2 Cosec ((38.65/2) +(34.43/2))
   = 431.80+1219.2 Cosec (19.32+17.21)
   = 431.80+1219.2(1/(sin (36.53))
   = 2480.05 mm
5. Steering Ratio:
   r = angle turned by the steering wheel/angle turned by the wheel
   = 45°/38.65°
   = 1.16
   Hence, the Steering Ratio will be 1:1
6. Max Steering Effort (E):
   E= Vertical load of tires/Steering ratio
   E= 72/1.16
   = 62.06 N
7. Tie rod length = 304.8 mm

8. Normal Force on Stub Axle (N):
   N= m*g
   = 72*9.81
   = 706.32 N
9. Tractive Force on Stub Axle:
   t = 706.32*Co-efficient of Friction
   = 0.6x706.32
   = 423.792 N

Table -1: Steering calculations results

Track width (front)	863.6 mm
Wheelbase	1219.2 mm
Ackermann angle	19.50°
Inner steer angle	34.43°
Outer steer angle	38.65°
Actual turning radius	2480.05 mm
Steering ratio	1.16:1
Max steering effort	94.7 N
Tie rod length	304.8 mm
Normal force on stub axle	706.32 N
Tractive force on stub axle	423.792 N
Steering wheel lock angle	45°

5. BRAKING SUBSYSTEM

The purpose of the braking system is to stop the vehicle in the shortest amount of time feasible. To do this, the vehicle's kinetic energy is changed into thermal energy, which is released into the atmosphere. Generally, in go-karts, a hydraulic braking system is used. which works on the principle-based on Pascal's law. When the brake pedal is pressed, brake fluid from the master cylinder enters the caliper through pipelines by the force of the piston. Due to the liquid force, the pistons of the caliper pushed away which in turn pushes the pads against a rotating disc, due to friction between pads and disc the rotating disc tend to stop. Hence braking takes place.
Now when the pedal is released, the piston of the master cylinder moves backward and fluid from the caliper to the master cylinder through the check valve.
Since the brake disc is a primary component of braking subsystem. The optimal design of disc is required

5.1 Braking calculations

Pedal ratio = L2 / L1 = 6/1 = 6
Where:
L1 =distance from the brake pedal arm pivot to the output rod clevis attachment
L2 =distance from the brake pedal arm pivot to the brake pedal pad

force applied on pedal by the driver (F) = 70 pounds (assume)
= 70*4.44
= 310.8 N
Pedal force generated (F_p) = F*Pedal ratio
= 70*4.44 x 6
= 1864.8 N

1. Pressure generated by master cylinder
Diameter of master cylinder piston (D_m) = 0.01905 m
Area of master cylinder piston (A_m) = $(\pi/4) * D_m{}^2$
= $2.849 * 10^{-4}$ m^2
Pressure generated by the master cylinder (P_m) = F_p / A_m
= $1864.8 / 2.849 * 10^{-4}$
= 6.543 MPa

2. Force exerted by the caliper
Diameter of caliper piston (D_c)= 0.032 m
Area of caliper piston (A_c) = $(\pi/4) * D_c{}^2$
= $8.04*10^{-4}$ m^2
Pressure transmitted to caliper (P_c)= 6.543 MPa
Force exerted by caliper (F_c)= P_c*A_c*no of pads
= $2*6.543*10^6*8.04*10^{-4}$
= 10521.144 N
Frictional force = F_c * coefficient of friction b/w rotor & pads
= 10521.144 * 0.4
= 4208.46 N

3. Torque on the rotor:
Torque on rotor = frictional force * effective radius of rotor
= 4208.46*0.072
= 303.016 N-m

4. Force acting on the wheel:
Torque on wheel (T_w) = Torque on rotor (T_r)
= 303.016 8N-m
Force acting on wheel = (T_w× coefficient of friction)/effective radius of wheel

= (303.016*0.7) / (0.139*0.96)
=1589.562 N

5. Deceleration of vehicle in motion:
The deceleration of the vehicle will be equal to (a_v) = friction force /mass of the vehicle
=4208.46 /180
= 23.38m/s^2

6. Braking distance of vehicle:
The theoretical braking distance of a vehicle in motion can be calculated as follows:
Braking distance = (velocity of vehicle)^2/ 2a_v
= (13.888)^2 / (2*23.38)
= 4.12 m

7. Braking time of vehicle:
The theoretical braking time of a vehicle in motion can be calculated as follows:
Time = (velocity / deacceleration)
=13.888/ 23.38
= 0.6 sec

8. Thermal calculations
Kinetic energy of the vehicle at max speed
= mV^2
= (180 *13.888 ^{2})
= 17358.888 J

Brake power = Kinetic energy / Brake time
= 17358.888 / 0.6
= 28931.4816 W

Rubbing area on one side of the disc
=(π/4)*[(pad outer diameter)^2 – (Pad inner diameter)^2]
= (π/4) *[(0.135)^2 – (0.120)^2]
= 0.003 m^2
Total rubbing area= 0.003* 2 = 0.006 m^2

Heat flux (q) = brake power / Total rubbing area
= 28931.4816 / 0.00647
= 4821913.5 W/ m^2

Rise in temperature of the disc while braking
T = (0.527 *q *√ (brake time) / (√ (density* sp. heat * thermal conductivity) [consider stainless steel material]
= (0.527 *4465055.329 * √0.6) / √ (7500 *490 *114)
T = 244.48°C
Max temperature produced in the disc during hard braking
= 125.7 + 30 (ambient temperature)
= 284.48°C

Table -2: Braking calculations results

Pressure acting on rotor	6.543 MPa
Clamping force	10521.144 N
Torque acting on rotor	303.016 N-m
Force acting on wheel	1589.562 N
Deceleration of vehicle	23.38 m/s^2
Stopping distance	4.12 m
Stopping time	0.6 sec
Total heat flux	4821913.5 W/ m^2
Maximum temperature	284.48^0 C

6 RESULTS AND DISCUSSIONS

6.1 Design and analysis of old stub axle and arm

For the steering sub-system, the stub-axel is designed and analyzed to get the perfect Ackermann steering mechanism [7], which makes the kart skid easily and allows to make a perfect Autocross and maneuverability.

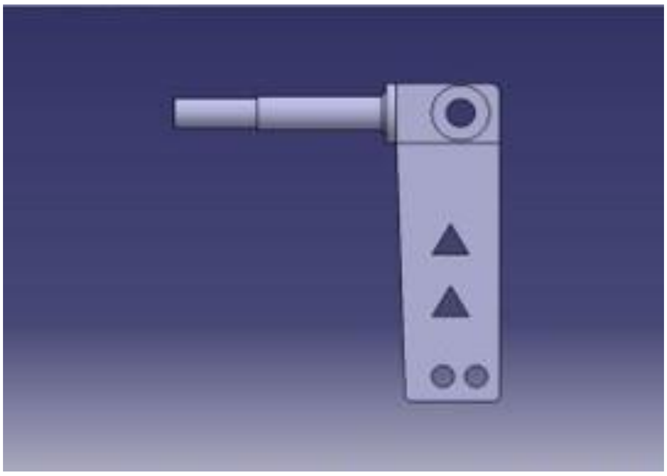

Fig -3: Old design of Stub axle

Structural analysis is performed on the old design of stub axle and stub arm, in order to find out the total deformation, stress concentration, and elastic strain in ANSYS 16.0.

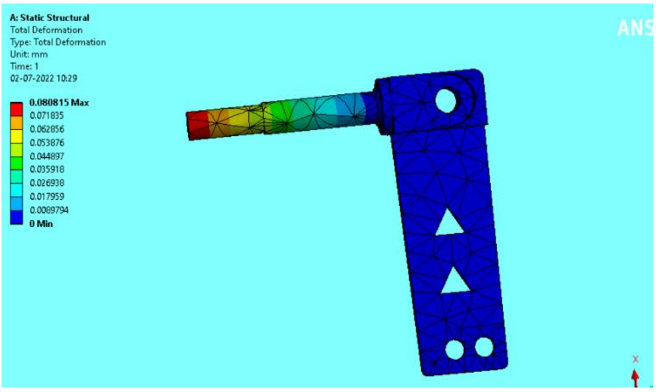

Fig -4a: Total deformation of old stub axle

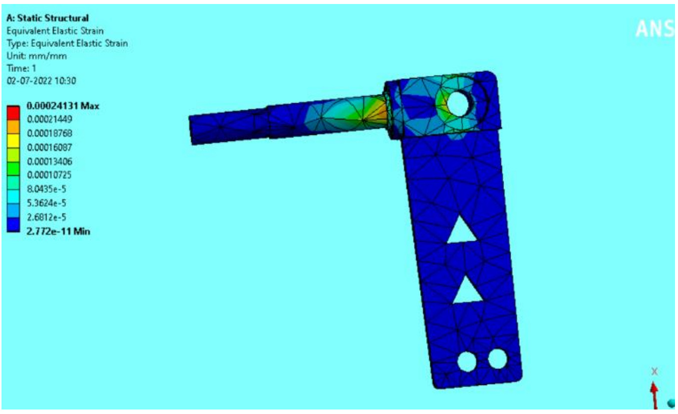

Fig -4b: Equivalent elastic stain of old stub axle

International Journal of Scientific Research in Engineering and Management (IJSREM)
Volume: 06 Issue: 07 | July - 2022 Impact Factor: 7.185 ISSN: 2582-3930

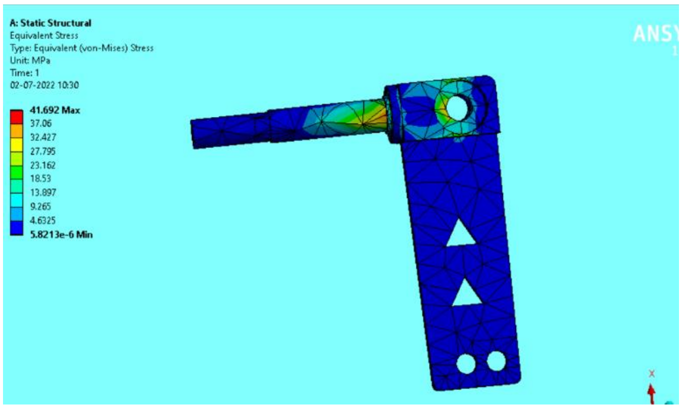

Fig -4c: Equivalent stress of old stub axle

Figures 4a, 4b & 4c shows the Structural analysis of stub axle of total deformation, equivalent elastic strain and equivalent stress. stub axle act as a cantilever beam when it is fixed.so the deformation is more at the free end of the stub axle. 0.0808 mm of deformation occurred when the load of 706.32 N is applied. The equivalent elastic strain generated due to the load applied is $0.2*10^{-3}$. Stress concentration is more at the change in cross-sectional area and the maximum stress concentrated at that point is 41.692 MPa.

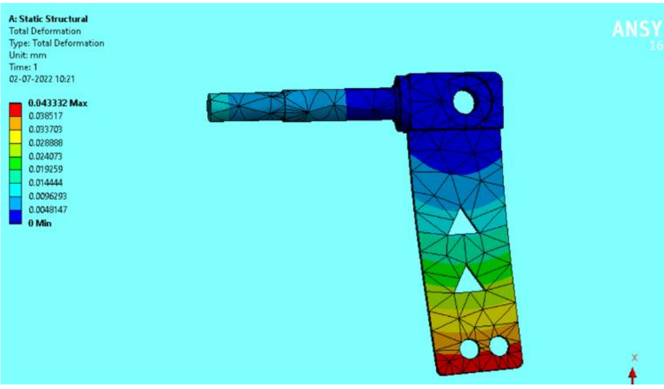

Fig -5a: Total deformation of old stub arm

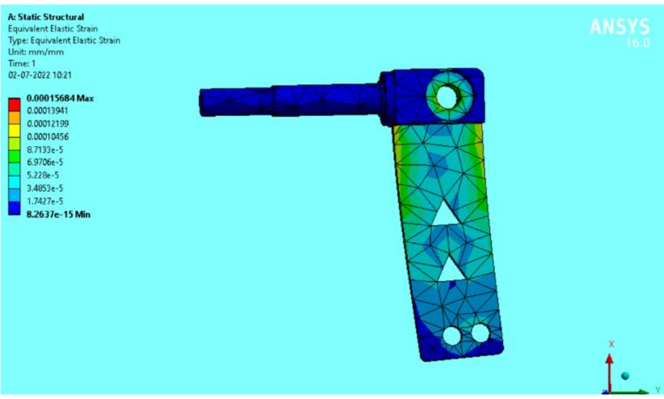

Fig -5b: Equivalent elastic strain of old stub arm

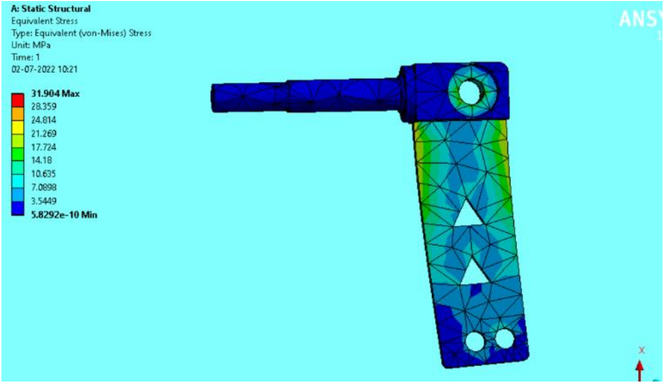

Fig -5c: Equivalent stress of old stub arm

Figure 5a,5b & 5c shows the Structural analysis of stub arm. In this the stub arm act as a cantilever beam, when the stub axle end is fixed so the deformation is more at the free end. It is observed that 0.04 mm of deformation occurred when the load of 423.792 N is applied on stub arm. The equivalent elastic strain generated due to the load applied is $0.1*10^{-3}$, and the maximum stress generated is 31.904 MPa.
As per the results of the analysis, the design is safe. But this stub axle design didn't form perfect Ackermann geometry due to the change in angle between stub axle and stub arm which in turn raised the problems mentioned in topic 3.1. Hence the design of the stub axle is optimized to get a perfect Ackermann geometry and the dimensions of the stub arm are reduced in order to reduce the weight.

6.2 Optimized design and analysis of stub axle

The angle required between the stub axle and stub arm is measured by considering the perfect Ackermann geometry and the angle obtained is 74°

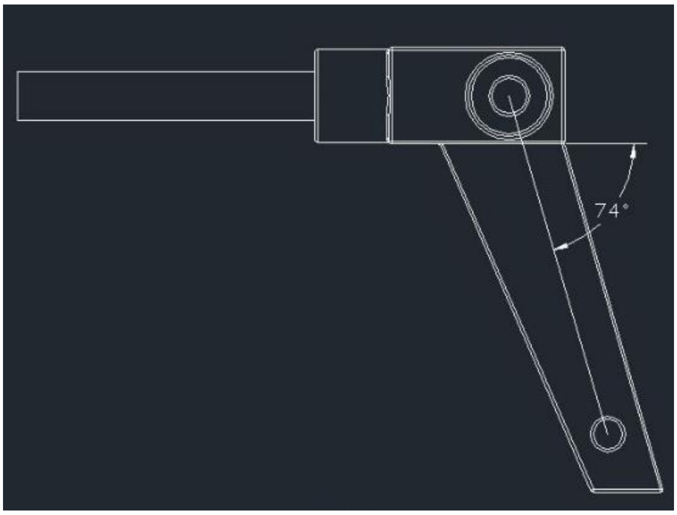

Fig -6: Sketch of the new optimized Stub axle

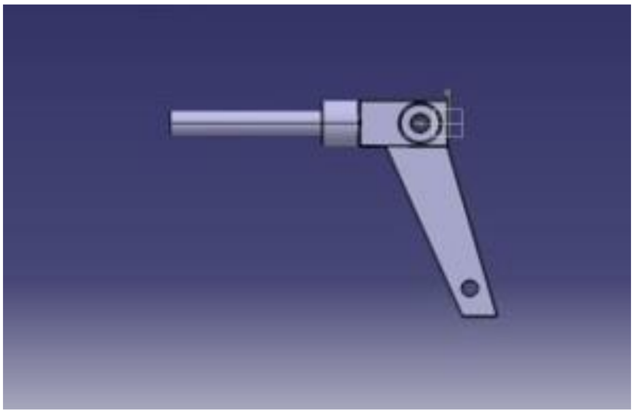

Fig -7: optimized design of Stub axle

Structural analysis is performed on the optimized design of the stub axle and stub arm, in order to find out the total deformation, stress concentration, and elastic strain, in ANSYS 16.0 software.

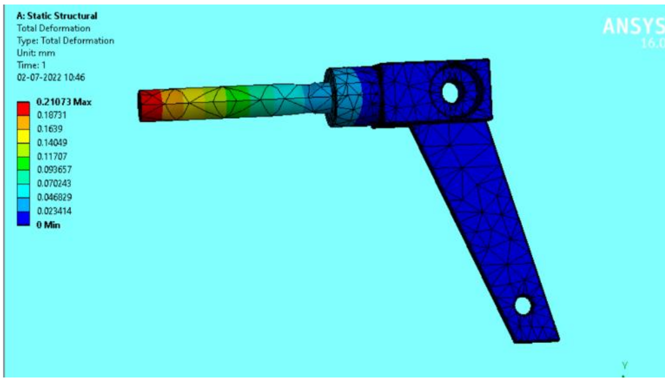

Fig -8a: Total deformation of new stub axle

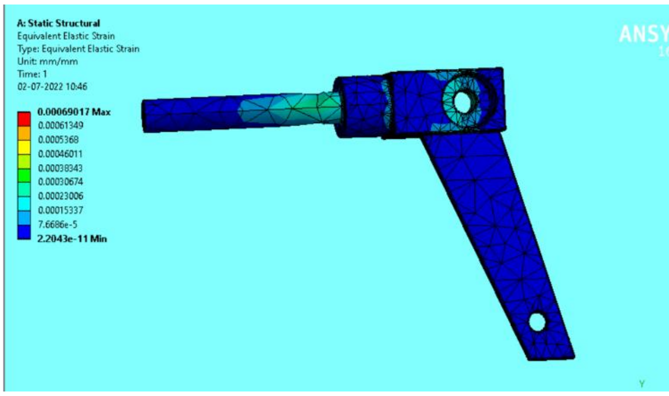

Fig -8b: Equivalent elastic stain of new stub axle

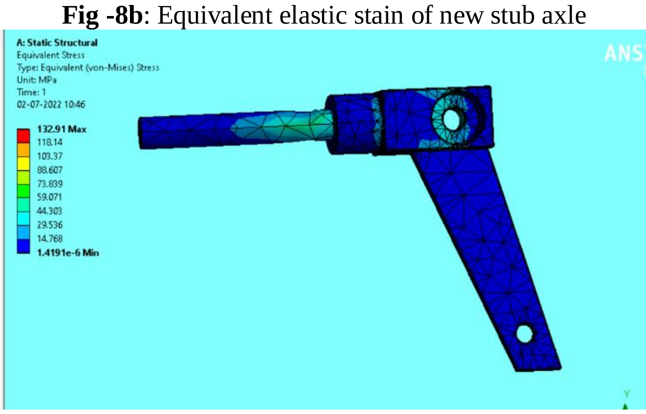

Fig -8c: Equivalent stress of new stub axle

Figure 8a, 8b & 8c shows the Structural analysis of stub axle The results shows that the maximum deformation occurred as 0.21 mm when 706.32N of load applied and this load acts at the end of the arm, at the same time the equivalent strain generated due to this load is $0.6*10^{-3}$, and stress generated is 132.91 MPa.

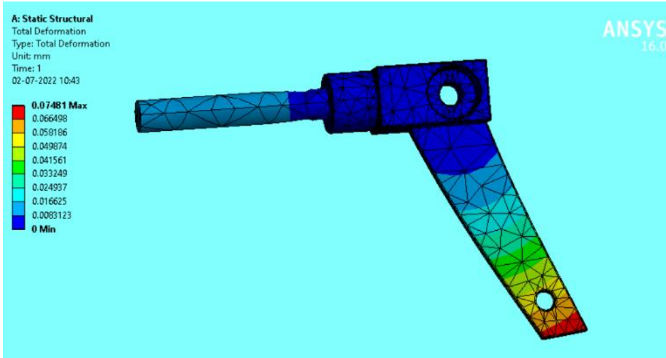

Fig -9a: Total deformation of new stub arm

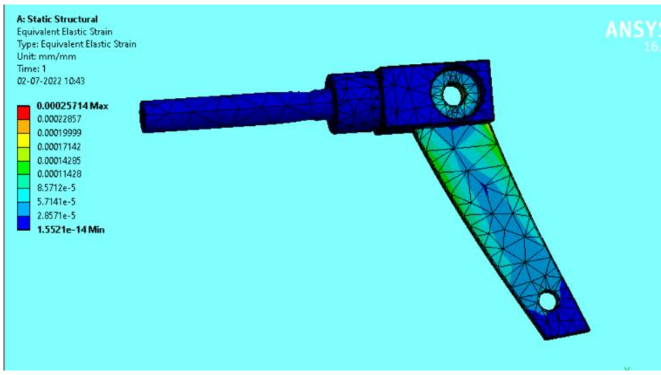

Fig -9b: Equivalent elastic stain of new stub arm

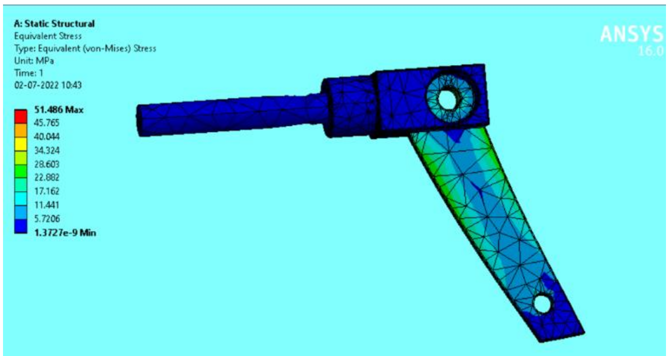

Fig -9c: Equivalent stress of new stub arm

figures 9a ,9b & 9c shows the Structural analysis of stub arm, 0.074 mm of deformation occurred when the load of 423.792 N is applied on the stub arm. The larger deformation occurred at the end of the arm because it acts as a cantilever beam. The equivalent elastic strain generated due to the load applied is $0.2*10^{-3}$, and the maximum stress generated is 51 MPa. The design is safe and the required angle is obtained and even the size of the stub arm is also reduced which in turns reduces the weight of the stub axle.

6.3 Design and analysis of old brake disc

The diameter of this disc shown in Figure 10 is 180mm and was designed using CATIA V5 software [7]. Structural analysis is performed on the brake disc in order to find out the total deformation, stress concentration, and elastic strain, in ANSYS 16.0 software.

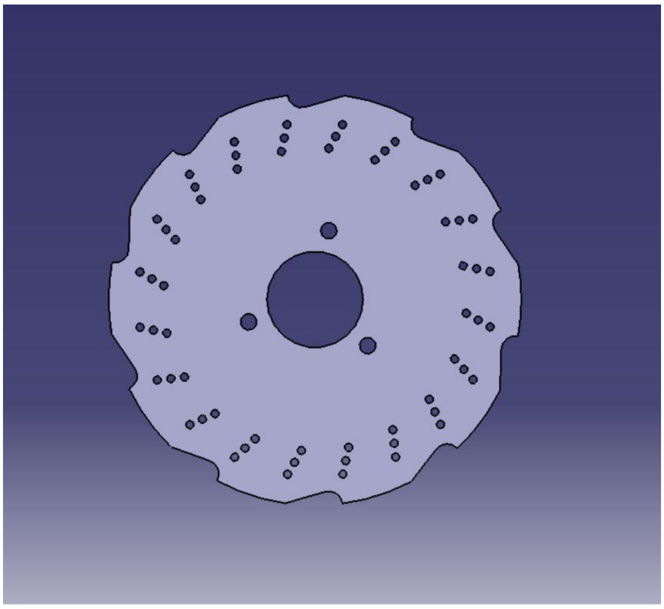

Fig -10: Old design of brake disc

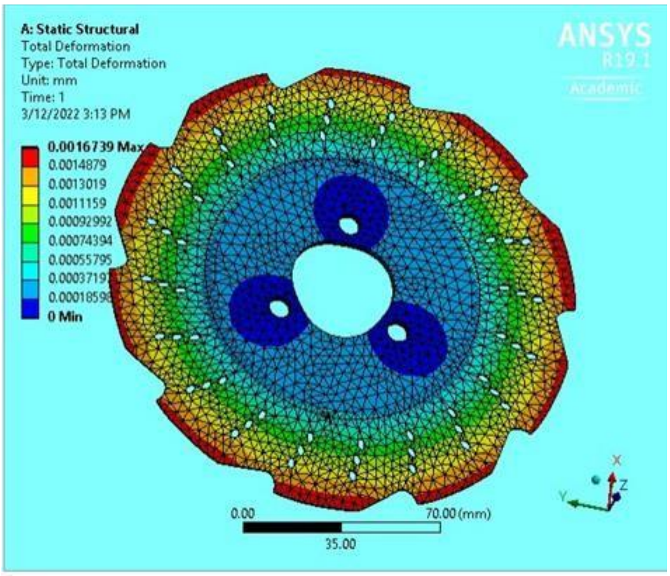

Fig -11a: Total deformation of old brake disc

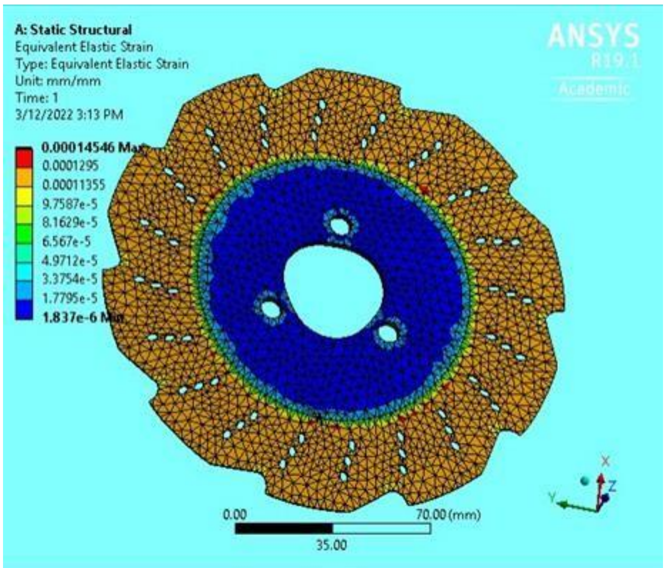

Fig -11b: Equivalent elastic stain of old brake disc

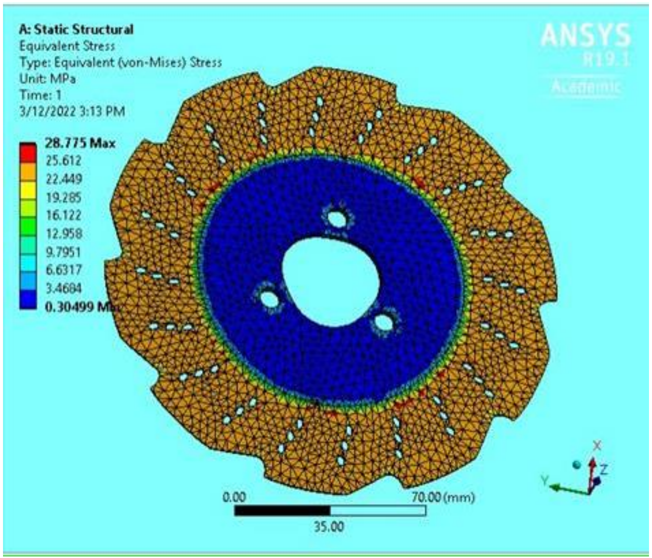

Fig -11c: Equivalent stress of old brake disc

Figures 11a, 11b & 11c shows Structural analysis of old brake disc. It is observed that the total deformation occurs at the effective radius of the brake disc, because the clamping force acts at this region. 0.0016 mm of deformation occurred when the pressure of 6.543 MPa is applied on brake disc. The equivalent elastic strain generated due to the load applied is $0.14*10^{-3}$, and the maximum stress generated is 28.77 MPa.

As per the results of analysis, the design is safe. But, due to the over size of the disc the ground clearance is becoming less than 1 inch which is not preferable for go-karts. Hence the design is optimized.

6.4 Optimized design and analysis of brake disc

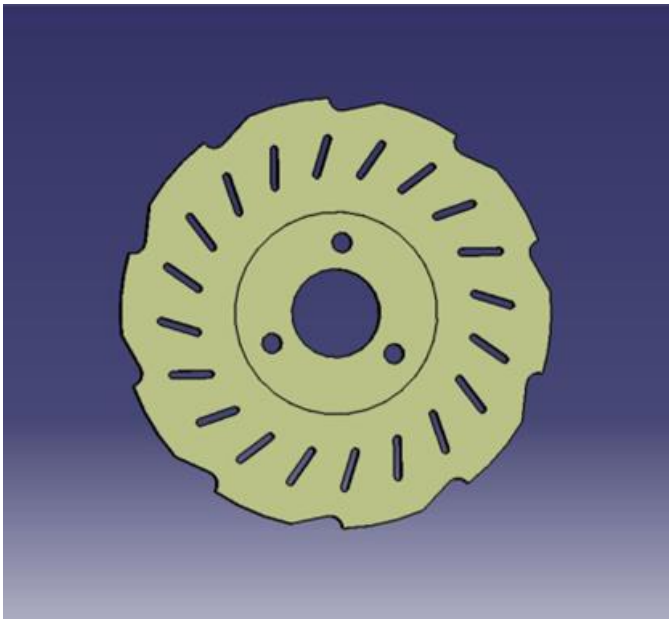

Fig -12: Optimized design of brake disc

The diameter is reduced to 150mm and a new brake disc is designed by making small changes in the profile. Structural analysis is performed on the optimized design of the brake disc, in order to find out the total deformation, stress concentration, and elastic strain, in ANSYS 16.1 software.

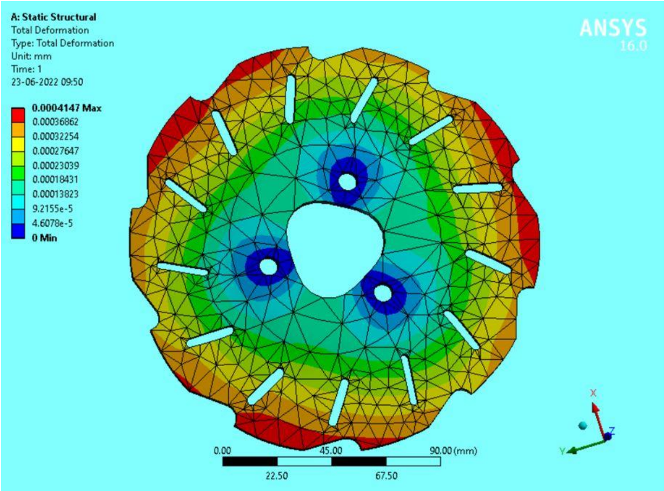

Fig -13a: Total deformation of new brake disc

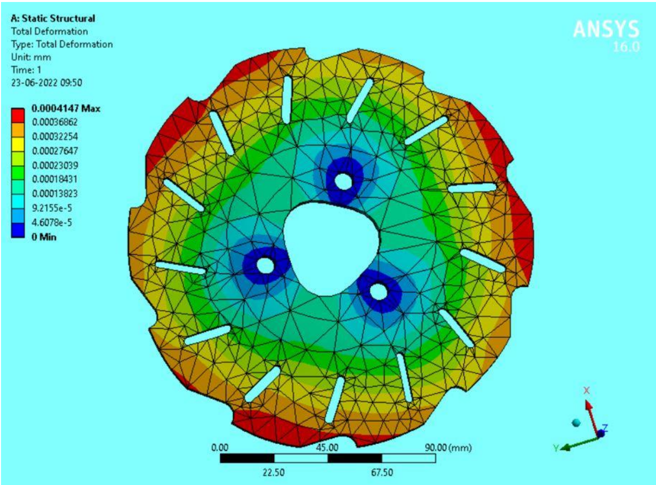

Fig -13b: Equivalent elastic stain of new brake disc

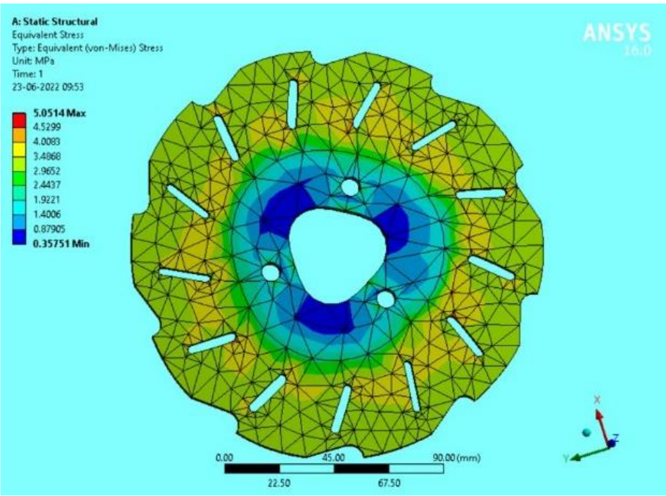

Fig -13c: Equivalent stress of new brake disc

Figure 13a, 13b & 13c shows the structural analysis on the brake disc. 0.0004 mm of deformation occurred when the pressure of 6.543 MPa is applied on the brake disc. The equivalent elastic strain generated due to the load applied is $2*10^{-5}$, and the maximum stress generated is 5.02 MPa. As per the results of the analysis, the design is safe. And has no effect even after changing the profile.

Now the optimized disc is analyzed for thermal analysis.

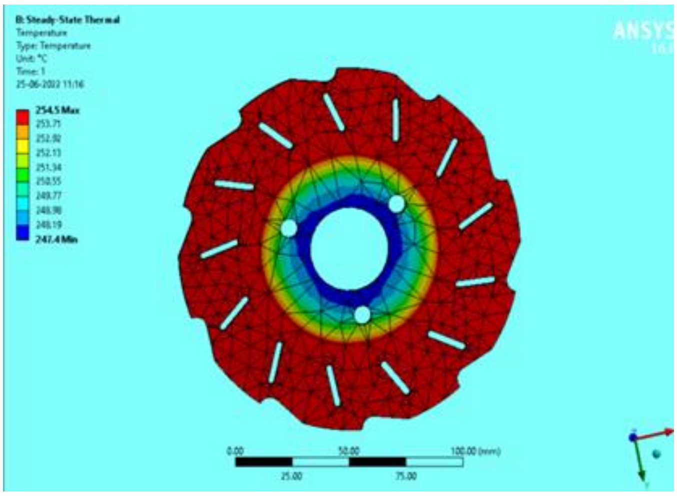

Fig -14a: Total heat flux of new brake disc

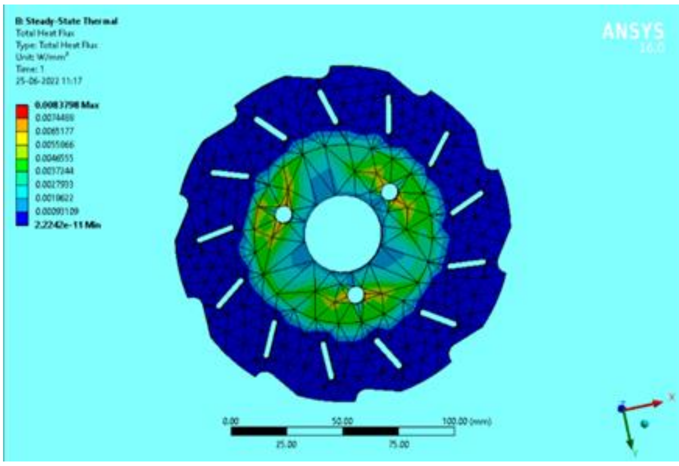

Fig -14b: Temperature distribution of new brake disc

Figures 14a & 14b shows the Thermal analysis of new brake disc. As the pressure is applied on effective area of brake disc. The kinetic energy of the brake disc is converted into heat energy in order to stop the disc rotation. The heat flux generated is more at that region and gradually decreases with the decrease in the diameter of the brake disc, due to natural air convection.

The design is safe and required ground clearance is achieved by decreasing the brake disc diameter.

7. CONCLUSIONS

By altering the stub-axle design and running a structural analysis on that developed design in ANSYS 16.0 software, the goal of constructing an efficient steering system to obtain optimal Ackermann geometry for a go-kart is achieved. The Design has achieved the shortest turning radius, which is 1.6 meters, and has been validated under dynamic conditions. And coming to the braking system, numeric computations have been done to obtain braking forces, braking torque, clamping forces at calipers, brake bias, and other important parameters. To determine the maximum heat flux and temperature, thermal calculations are performed. According to theoretical calculations, optimization in the design of the brake disc is carried out, and a new brake disc is created in the CATIA software. Results of a disc plate's linked steady-state thermal and static structural study performed in ANSYS 16.0 are presented. These outcomes are quite encouraging, which confirms the viability of our brake system.

REFERENCES

1. Masood M, Appam Nihar, Syed Najam Ali, Mohd Sayeed “Braking system of Go-kart”. International Advanced Research Journal in Science, Engineering and Technology Vol.4, Issue 5, May 2017.
2. V.K. Saini, Sunil Kumar, Amit Kumar Shakya, Harshit Mishra, “Design methodology of Steering system for All-Terrain Vehicles”. International Research Journal of Engineering and Technology Vol.4, Issue 5, May 2017.
3. Mohd Anwar, Ashraf Shaik, Mohd Sohail “Steering system of Go-kart”. International Advanced Research Journal in Science, Engineering and Technology Vol.4, Issue 5, May 2017.
4. Aditya Kolakoti, T V K Bhanuprakash, H N Das. CFD analysis of controllable pitch propeller used in marine vehicle. Global Journal of Engineering Design and Technology. (2013), 2(5), 25-33.
5. Aditya Kolakoti and B V Appa Rao. System and method for a supercharged IDI engine run by biodiesel. Indian Patent. (2017), Patent No. 201741014482.
6. Kolakoti, Aditya and Metta, Raghu and Siddhartha Yadav, J, Thermodynamic Analysis of Various Heat Loss Factors from a Diesel Engine Fueled with Neat Biodiesels (2021). Available at SSRN: https://ssrn.com/abstract=3873706 or http://dx.doi.org/10.2139/ssrn.3873706
7. Kolakoti, Aditya, Panchanand Jha, Prakasa Rao Mosa, Manohar Mahapatro, and Tulasi Ganesh Kotaru. “Optimization and Modelling of Mahua Oil Biodiesel Using RSM and Genetic Algorithm Techniques.” Mathematical Models in Engineering 6, no. 2 (June 2, 2020): 134–46. https://doi.org/10.21595/mme.2020.21357.
8. Akshay Pawar, Suraj Zambare, “Design of steering system for All-Terrain Vehicles” International Research Journal of Engineering and Technology Vol.5, Issue 3, May 2018.
9. Satya Prakash Gupta, Gurudayal kumar[2] ”Braking system design for a Go-kart” Global Journal For Research Analysis Vol 7, Issue 2, Feb 2018
10. Sourav Patinaik “Design and analysis of Braking system for BAJA All-Terrain Vehicles” International Research Journal of Engineering and Technology Vol.7, Issue 2, May 2020.